



# Hotspots and Hot Moments of Metal Mobilization: Dynamic Connectivity in Legacy Mine Waters

Anita Alexandra Sanchez<sup>1,2\*</sup>, Maximilian P. Lau<sup>1,2</sup>, Sean Adam<sup>1,3</sup>, Sabrina Hedrich<sup>1,4</sup>, & Conrad Jackisch<sup>1,3</sup>

<sup>1</sup>Interdisciplinary Environmental Research Centre, Technische Universität Bergakademie Freiberg, Freiberg, 09599, Germany

<sup>2</sup>Institute of Mineralogy, Technische Universität Bergakademie Freiberg, Freiberg, 09599, Germany

<sup>3</sup>Institute of Drilling Technology and Fluid Mining, Technische Universität Bergakademie Freiberg, Freiberg, 09599, Germany

<sup>4</sup>Institute of Biosciences, Technische Universität Bergakademie Freiberg, Freiberg, 09599, Germany

*Correspondence to:* Anita Alexandra Sanchez (Anita.Sanchez@mineral.tu-freiberg.de)

**Abstract.** Monitoring and treatment of contaminated mine water conventionally focuses on end-of-pipe assessment and remediation techniques, at the downstream outlet of mining sites after closure. Conversely, the initial stages of pollutant release and their pathways within abandoned mines have been largely overlooked. This study examines subsurface mining-affected anthropogenic structures and the dynamic hydrogeochemical loadings and drainage pathways within them, revealing how variable subsurface flow activation impacts metal(loid) mobilization and opens novel direct mitigation options. We identified complex hydrological patterns through the mine (Reiche Zeche, Ore Mountains, Germany) in which percolation paths were dynamically connected to the drainage based on flow conditions. Using in-situ sensors, hydrogeochemical monitoring and stable water isotopes, we reveal a hydrodynamic regime in which episodic shifts in subsurface connectivity govern metal(loid) mobilization from localized storage zones, ultimately controlling solute export to surface waters. We use concentration–discharge (C–Q) relationships, hysteresis indices, and the Pollution Load Index (PLI) to evaluate metal transport during the annual pattern of flow regimes. Our analyses of event-scale C–Q hysteresis patterns reveal site- and element-specific shifts in flow path activation in a very short time. Despite low flow periods traditionally considered low risk for contaminant mobilization, contaminant hotspots within poorly connected hydrological zones can emerge during these times, with high pollution potential and solute accumulation governed by the sequence and timing of crossing or exceeding a connectivity or flow threshold, as described by the hydrological fill-and-spill and geochemical lotic-lentic cycle concepts. Notably, Zn loads during low flow, pre-flush periods reached levels up to six times higher than median values. Preceding the flushing events, geochemical and microbial-mediated metal leaching create the spatially distributed contaminant stock, remobilized during reconnection events. With a large proportion of heavy metal loads occur during low flow and especially just before the high flow (flush) period, source-related mitigation with decentralized water treatment structures becomes much more feasible than end-of-pipe solutions that require higher throughput volumes and multi-element filtering. This work also highlights the need for event-sensitive monitoring and treatment strategy options that prioritize internal system behavior to mitigate pollution risk in abandoned mines and other caverned hydrological systems.



## 1 Introduction

Metal mining has left a pervasive global legacy of water contamination, particularly in river basins downstream of historic and active metal extraction zones (Macklin et al., 2023; Sergeant et al., 2022). Mine drainage affects more than 23 million people and thousands of kilometers of rivers globally, with risks that span decades to centuries after mine closure (Macklin et al., 2025). Despite regulatory progress, abandoned mine sites often lack monitoring and management, leaving communities and aquatic habitats vulnerable to pollution pulses triggered by hydrological events or anthropogenic disturbances. Standard monitoring under the European Water Framework Directive (WFD) and conventional water quality assessments (LAWA, 2003) typically rely on infrequent, discrete measurements providing only limited snapshots of hydrogeochemical processes (Resongles et al., 2015).

The consequences are particularly evident in regions with long mining histories, such as the Ore Mountains of Central Europe. Here, as in many former mining areas, legacy pollutants from underground workings pose environmental threats long after extraction has ceased (Huang et al., 2023; Liu et al., 2014) for example in the form of diffuse and point-source runoff of acidic waters bearing high concentrations of metals and sulfates (Bozau and Liessmann, 2017; Haferburg et al., 2022). While much attention has focused on surface water systems downstream former mining sites, the internal hydrogeochemical dynamics of underground mine workings remain poorly understood, especially in relation to episodic contaminant mobilization and non-conservative transport (Hudson et al., 2018; Datta et al., 2016). Addressing these blind spots is critical for understanding pollution behavior in mining-impacted systems and for designing effective remediation strategies.

Despite visible surface effects, the contaminant sources and pathways within abandoned underground mines remain largely obscured. Seeping waters infiltrate the mining system through complex pathways along underground waste rock deposits. The pools and pathways contributing to mine water pollution are therefore numerous, and due to the limited accessibility, largely understudied. The waters that dissolve and transport various elements while percolating through a fractured system suggest that pollution is not created continuously and diffuse but instead governed by discrete, intermittent and dynamically connective pathways. With hydrologic connectivity (Freeman et al., 2007) and intermittency (Fovet et al., 2021) known to impose specific characteristics on water-mediated transport and turnover in soil and other environments (Turnbull et al., 2018), the hydrological processes underlying contaminant mobilization and dispersal in abandoned mines may be better described using the tools and concepts such as phases of fill-and-spill (McDonnell et al., 2021) or lotic-lentic cycles (Schmadel et al., 2018).

In natural hydrologic systems, drainage connectivity, which controls water and solute transport, is shaped by catchment topography and becomes activated under specific hydro-meteorological conditions such as antecedent moisture, precipitation, infiltration, and subsurface flow through soil and fractured rock (Knapp et al., 2020; Li et al., 2017; Musolff et al., 2017; Lemenkova et al., 2021). In mining systems, near-surface signals are often dampened by deep storage and low percolation, making hydrological responses lagged, low-pass filtered and threshold-dependent. Given the dispersed flow paths through subsurface waste rock deposits and other anthropogenic preferential flow paths, various fill-and-spill pools overlay. To



decipher the diffuse source pattern, the closer the analysis can get to the individual sources and the higher the temporal resolution, the clearer should the mobilization pattern be revealed.

Stable water isotopes ( $\delta^2\text{H}$ ,  $\delta^{18}\text{O}$ ) are useful tracers for identifying flow paths, water pool mixing, and water-rock interactions (Sprenger et al., 2016; Spangenberg et al., 2007; Clark and Fritz, 2007; Kumar et al., 2024). Though widely used in ecohydrology, isotopic tools remain underutilized in mine drainage studies. We suggest that they could provide a promising means of tracing complex contaminant sources and transport processes (Ghomshei and Allen, 2000; Allen and Voormeji, 2002; Hazen et al., 2002).

The influence of extreme events and episodic flushing is widely recognized in surface catchments, but similar mechanisms in mine systems are poorly characterized. Direct reactions to surface storm events are very rare (Burnt et al., 2025). Instead, subsurface flood events following sufficiently wet periods can mobilize accumulated contaminants during their initial stages, producing a first-flush effect in which solute concentrations peak early before declining, as dilution or source depletion sets in (Merritt and Power, 2022; Bryne et al., 2012). This early surge is typically linked to the rapid mobilization of readily accessible contaminant stores located near the water interfaces, such as secondary mineral phases and fine sediments. These materials are easily entrained once hydrologic thresholds are crossed (e.g., rising water tables or shear stress increases) are crossed, leading to a sharp but short-lived release pulse (Resongles et al., 2015).

Concentration-discharge (C-Q) relationships offer a powerful tool to describe such flow-phase-dependent behavior and have seen broad application in watersheds (Shaw et al., 2020; Rose et al., 2018; Godsey et al., 2009; Knapp et al., 2020). In C-Q analysis, when solute concentrations remain stable despite changes in discharge, chemostatic behavior is observed, often linked to proportional weathering increases (Godsey et al., 2009; Li et al., 2017) and homogeneous solute distribution (Herndon et al., 2015). In contrast, when concentrations increase (enrichment) or decrease (dilution) with discharge, chemodynamic behavior reflects heterogeneous solute distribution associated with geologic units within a watershed (Herndon et al., 2015). Applying C-Q analysis in underground systems remains minimal, representing a methodological gap this study seeks to address.

C-Q slopes reveal the overall export regime for each metal (Fig. 1a). Positive slopes reflect enrichment, typically associated with transport-limited mobilization when water flow conditions control delivery (Balerna et al., 2021), while negative slopes indicate dilution, consistent with source-limited conditions when mobilization is constrained by availability. Hysteresis patterns reveal time lags between discharge and concentration, offering insights into hydraulic connectivity (Pohle et al., 2021) and mobilization processes at large (Lloyd et al., 2016). Clockwise loops suggest rapid mobilization from proximal sources, while counterclockwise loops imply delayed transport from distal or disconnected zones (Fig. 1b, Rose et al., 2018; Pohle et al., 2021; Speir et al., 2024). Complex patterns suggest multiple or shifting sources and transport mechanisms. Linking discharge and chemistry to quantify metal loads helps identify contaminant sources and pathways (Kimball et al., 2002). By combining these diagnostic tools with connectivity-informed hydrological concepts, we aim to uncover the mechanisms that govern metal export from abandoned mine systems.

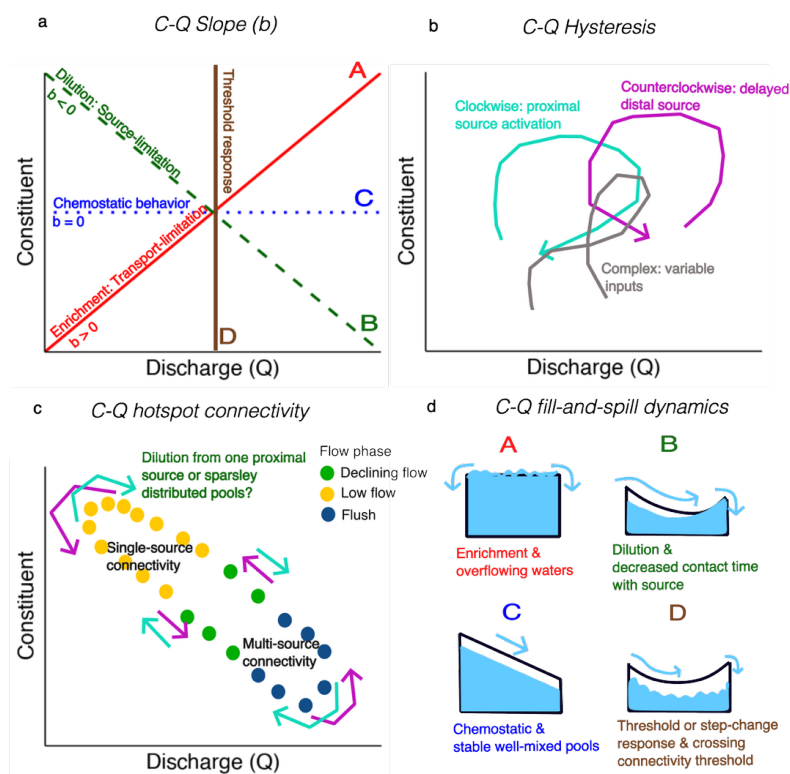


**Figure 1: Conceptual representation of four concentration–discharge (C–Q) relationships and their mechanistic interpretations. (a) Export regimes based on C–Q slope: dilution ( $b < 0$ ), chemostatic ( $b \approx 0$ ), and enrichment ( $b > 0$ ). (b) Hysteresis loop types reflecting solute transport timing: clockwise (proximal source activation), counterclockwise (delayed distal source), and complex (variable inputs). (c) C–Q responses through evolving hydrological connectivity from single-source (low flow) to multi-source (flush) mobilization. (d) C–Q patterns linked with fill-and-spill dynamics: A. *Enrichment*: Constituent concentrations increase with discharge, consistent with overflow-driven mobilization from previously disconnected sources. B. *Dilution*: Concentrations decrease with increasing discharge, reflecting increased water volume with limited solute input or reduced contact time with solute-rich sources. C. *Chemostatic*: Concentrations remain constant across a range of flows, suggesting a well-mixed reservoir with stable release conditions. D. *Threshold response*: A sudden shift in concentration at a specific discharge value, indicating step-change behavior such as activation of a new flow path or crossing a connectivity threshold.**

Flow response analyses do not preclude the mechanistical underpinnings of contaminant supply to flowing waters. The speciation and abundance of contaminants in mine drainage is governed by pH, redox potential, and the interaction of different water sources, which collectively control solute behavior and contaminant loads (Shaw et al., 2020). Observing dynamics through a connectivity-mediated lens (Fig. 1c) can elucidate characteristics beyond general percolation. These flow-phase transition behaviors are best understood through the fill-and-spill concept in which water accumulates in isolated pools until a threshold is reached, after which overflow activates previously disconnected pathways (McDonnell et al., 2021). Depending



115 on timing and connectivity, a period of high spillage may or may not coincide with elevated contaminant loads. Figure 1d  
synthesizes these relationships, emphasizing how flow-phase transitions and episodic connectivity shape contaminant export  
and generate hotspots of locally intensified metal release (Vidon et al., 2010) and hot moments of intensified metal discharge.  
These phenomena are rarely monitored in mines, yet are likely central to understanding temporal variability in contaminant  
export.

120 Building on our previous study that identified strong spatial and temporal heterogeneity in contaminant release within the  
Reiche Zeche mine (Sanchez et al., 2025), we test the capability of high-resolution complementary methods to identify hotspots  
and hot moments of pollution in fractured, legacy mine water networks. We seek to resolve the internal drivers of contaminant  
release within the mine, providing the mechanistic understanding required for adaptive, near-source treatment. In the present  
work, we do this by addressing two central research questions: (1) how can dynamic contaminant mobilization be monitored  
125 effectively within an underground mine environment, and (2) how do these dynamics inform treatment strategies beyond  
conventional end-of-pipe approaches? We hypothesize that alternating hydrological flow phases control dynamic connectivity  
and thus metal mobilization, with C-Q patterns revealing the behavior of localized pools within the mine.

For over two years, we performed 42 sampling campaigns and utilized in-situ sensors across four distinct flow paths. At one  
site, we conducted high-resolution and high-frequency monitoring using an in-situ UV-Vis spectrometer to capture transient  
130 fluctuations. Our primary objectives were (1) to characterize the temporal evolution of flow regimes and their influence on  
contaminants, (2) to determine the geochemical signatures associated with localized pools, and (3) to assess how different flow  
phases affect C-Q behavior and solute loads. To address our research questions and hypotheses, we integrate multi-scale  
hydrogeochemical monitoring with event-sensitive methods, applying tools commonly used in surface hydrology, such as C-  
Q relationships and hotspots/hot moments, and apply them to an underground mine drainage system. Ultimately, this study  
135 contributes a transferable framework for diagnosing contaminant risks in legacy mine settings and supports the development  
of adaptive, near-source water treatment strategies.

## 2 Methods

### 2.1 Study site and sample collection

Situated in the Ore Mountains of Central Europe, the historic Reiche Zeche mine site, 50.928° N 13.357° E, is one of the many  
140 old mines whose runoff flows untreated into streams that feed the Elbe river, one of the largest rivers in Europe (LfULG,  
2014). This site was active in extracting high-grade minerals, specifically silver ore, and processing mine waste rock up until  
1969. Subsequently, the lower sections of the adit system, which extend down to 1300 meters, became inundated with water  
up to the level of the central adit “Rothschönberger Stollen”, which is 250 meters below the surface at the Reiche Zeche mine  
shaft (Zhiteneva et al., 2016; Mischo et al., 2021). The mine now represents a flooded, multi-level system with complex  
145 subsurface flow pathways. This hydrological complexity, dispersed flow above extraction levels and preferential flow through  
waste deposits, makes the site ideal for addressing our research questions.



This study focuses on a single slanted vertical extraction structure which spans over three levels before reaching the central drainage adit (Fig. 2). These levels include: Level 1 (located 103 meters below the surface); Level 2 (149 meters below the surface); and Level 3 (191 meters below the surface). A total of 26 sites were selected for ongoing sampling, but four specific sites will be in the focus. The four locations, sites 1, 2, 3A, and 3B, were selected due to the presence of continuous and ample amounts of flowing water in comparison to the rest of the locations which were not as great in volume of flowing water. In one-to-three-week intervals, we conducted 42 sample campaigns to all sites from February 3<sup>rd</sup>, 2022 to May 31<sup>st</sup>, 2024. All data are reported in the B2SHARE Data Repository (Sanchez et al., 2025b).

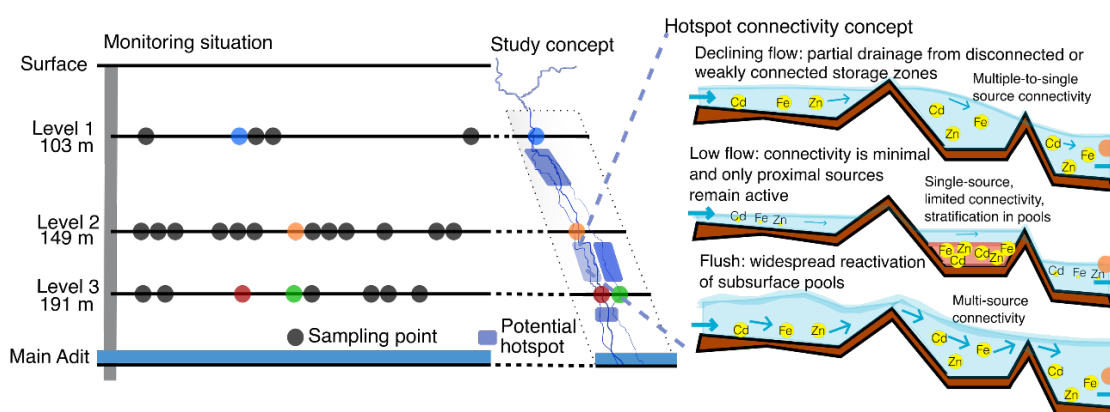


**Figure 2: Conceptual framework and study layout of the abandoned mine system levels above the main adit at Reiche Zeche. Left: monitoring locations across three mine levels, with four sites (1, 2, 3A, 3B) selected for high-frequency sampling. Instrumentation at all four sites included flow loggers, with additional high-frequency sensors and an autosampler deployed at site 2 for a 10-month intensive monitoring period. Middle: concept of site placement along flow path through the mine and associated contaminant hotspots (blueish purple zones). Potential hotspots along the flow paths to sites 3A and 3B are depicted in different color shades to emphasize their distinct source zones, despite spatial proximity to site 2. Right: conceptual model of flow-phase-dependent fill-and-spill connectivity. Blue arrows represent flow direction; shaded red areas indicate stratification. Flow regimes govern activation of solute source zones, resulting in distinct connectivity patterns.**

## 2.2 Sampling design and conceptualization of site-specific dynamics

To unravel the internal dynamic hydrogeochemical characteristics of the abandoned ore mine and to interpret observed heterogeneity in space and time, we focused on four strategically selected sites (1, 2, 3A, and 3B) that consistently exhibited sufficient water flow for high-frequency monitoring. These sites span across three levels of the mine, enabling a vertical profile of hydrological connectivity within the system (Fig. 2). Over two years of sampling, we tracked discharge, isotopic composition ( $\delta^2\text{H}$  and  $\delta^{18}\text{O}$ ), and dissolved metal(loid) concentrations at 26 locations (Fig. 2 and Table S1). Initial observations



revealed strong spatial heterogeneity in metal(loid) concentrations (Fig. S1) and dynamic flow variability, which suggests the presence of transient contaminant hotspots and episodic connectivity. To interpret these patterns mechanistically, we developed a hotspot connectivity concept grounded in the fill-and-spill paradigm (Fig. 2, right panel). This framework illustrates how flow-phase-dependent changes in hydrological connectivity control source zone activation. Similar to braiding rivers, we expect parts of the system as being always drained and an increasing number of adjacent pools becoming connected with increasing water flow (Wilson et al., 2024). Permanently spilled sections have rather low metal(loid) concentrations, while temporarily disconnected sections act as niches for microbially mediated solving and hence elevated metal(loid) concentrations (Sanchez et al., 2025).

The Central European hydrological cycle (wet winters, dry summers) produces three recurring drainage phases in the mine: flush (high flow), declining flow, and low flow. During low flow, hydrological disconnection allows solutes to accumulate in lentic or weakly connected storage zones. Flush events re-establish connectivity, linking multiple pools and triggering contaminant release (Sanchez et al., 2024), while declining flow reflects waning but still active transport. Stratification during low and declining flows (Fig. 2) acts as a critical disconnection mechanism that can delay or abruptly initiate solute mobilization.

Although sites 2, 3A, and 3B are located on the same mine level, they receive water from distinct source zones shaped by geological structure, mining voids, and fracture networks. These differences lead to divergent C–Q dynamics and hysteresis patterns, reflecting contrasts in pool storage, reconnection timing, and redox conditions. Such site-specific variability underscores the need to analyze contaminant transport at multiple locations within the mine.

### 2.3 Hydrological data collection and analysis

To understand whether surface hydro-meteorological forcing translates into episodic contaminant release underground, we monitored both external conditions and internal mine discharge. Meteorological conditions are monitored in an automated station at the surface next to the central access shaft to the Reiche Zeche research and education mine. To avoid more complex hydrological modelling, a standardized water availability index, i.e. the Self-Calibrating Palmer Drought Severity Index (PDSI), was used to characterize the overall moisture conditions of the system and pre-event wetness levels (Wells et al., 2004; Palmer et al., 2016). The drought index values are determined by using reference potential evapotranspiration (FAO56 Penman-Monteith method) and precipitation data, and a simplified soil water balance model. The magnitude of PDSI indicates the severity of the departure from normal conditions. A PDSI value greater than 1 represents wet conditions, while a PDSI value less than -1 represents dry conditions at the surface. The general dry and wet phases from the surface were compared with flow rate measurements from within the mine.

Continuous water level and flow monitoring was conducted at four sites within the Reiche Zeche mine using pressure sensors (Levellogger5, Solinst Georgetown) between February 2022 to March 2024. Sites 1 and 2 were equipped with plastic weirs for discharge measurement, while the existing carved spillways were used at sites 3A and 3B. Site-specific water level-discharge



relationships were established (Henderson, 1966) and the resulting flow time series were smoothed using a Savitzky-Golay  
205 filter.

Additionally, to distinguish between recharge and stored drainage contributions, water stable isotopes ( $\delta^2\text{H}$  and  $\delta^{18}\text{O}$ ) were  
analyzed via cavity ring-down spectroscopy (L-2130i, Picarro Santa Clara) to trace water sources (See SI for details on  
discharge calculations and isotope methods). Comparison with the local meteoric water line (LMWL) and calculation of an  
offset from the general background concentration (centroid of all samples) and between the stations were used to assess  
210 seasonal recharge and drainage contributions and distinguish between precipitation-dominated and older subsurface waters.

## 2.4 Physico-chemical data collection and analysis

To evaluate contaminant concentrations and solute composition, we combined field parameters with laboratory analyses. Acid-  
washed HDPE bottles, pre-rinsed with deionized water, were used to collect water samples. For all samples, pH and  
215 conductivity were measured (pH 340 and Cond 3310 sensors, WTW Weilheim). Prior to conducting analyses for dissolved  
organic carbon (DOC), dissolved inorganic carbon (DIC), and metal(loid)s, we filtered the samples using polyethersulfone  
filters with 0.45  $\mu\text{m}$  pores (Filtropur S, Sarstedt Nümbrecht). The DIC and DOC concentrations were measured in triplicate  
for each sample using a total organic carbon analyzer (TOC-L series, Shimadzu Duisburg). For DOC measurements, we  
employed a high temperature combustion method, categorizing it as non-purgeable organic carbon (NPOC). This involved  
220 acidifying and then purging the samples with oxygen to expel inorganic carbon before the analysis. The precision of our data  
was validated by computing the standard deviation of the triple measurements, ensuring data reliability within the instrument's  
precision range (coefficient of variation < 2% and standard error < 0.1). We quantified metal(loid) concentrations using  
inductively coupled plasma optical emission spectroscopy (ICP-OES Optima 5300 DV Spectrometer, PerkinElmer Rodgau).  
For metal(loid) analysis, we prepared the samples with an addition of 1 mL of 2M nitric acid and included the following  
225 metal(loid)s in our analysis: iron (Fe), zinc (Zn), arsenic (As), copper (Cu), cadmium (Cd), lead (Pb), aluminum (Al), nickel  
(Ni), and manganese (Mn). These parameters allowed us to assess both geochemical conditions and contaminant levels under  
varying hydrological phases.

## 2.5 Automated sampling and high-resolution monitoring

230 To capture short-lived contaminant pulses that campaign sampling might miss, we complemented discrete sampling with  
automated high-frequency monitoring at site 2. An autosampler (6712 Full-Size portable sampler, ISCO Nebraska) was  
positioned at this site from May 16<sup>th</sup>, 2022 to February 14<sup>th</sup>, 2023 as an approach to avoid missing unseen aspects in the  
temporal dynamics of mine drainage water quality. The autosampler was calibrated to take a sample daily. 21 out of 24 1-L  
autosampler bottles were each filled with 10 mL of 2 M HCl prior to each start of the autosampler run to stabilize the metal(loid)  
235 solutions for measurements in the laboratory, while three autosampler bottles (one every seven days) were unacidified to record  
accurate pH and electrical conductivity measurements. The autosampler was filled every three weeks and 250 mL samples  
were collected from each bottle in the machine. Samples were filtered in the lab and prepared for further analyses. Prior to



each new campaign, all 250 ml autosampler bottles were cleaned in a lab dishwasher and rinsed with deionized water. To complement this daily automated sampling, we submersed an online UV-Vis spectrometer probe (spectro::lyser V3, scan GmbH Vienna; in the following simply termed spectrolyzer) in the flow channel from May 16<sup>th</sup>, 2022 to May 23<sup>rd</sup>, 2023 to record hourly absorbance measurements over a wavelength range of 200 to 720 nm at 2.5 nm increments.

To analyze and compare the spectral data obtained from the spectrolyzer with the metal(loid) concentration data collected by the autosampler at site 2 over time, we employed Quinlan's Cubist modeling (Kuhn and Johnson, 2013). Cubist, a rule-based method using spectrometric measurements, combines decision trees with linear models at the leaves, allowing for the prediction of continuous numerical variables. This approach was suited to our study because it handles non-linear relationships while maintaining interpretability. The modeling framework was applied to all analyzed metal(loid)s (see SI for details), while here we highlight cadmium as an illustrative example.

## 2.6 Statistical and analytical framework

### 2.6.1 Hydrological phase classification

To evaluate the influence of hydrological and geochemical drivers on contaminant mobilization, we divided the time series into three hydrologically defined flow phases: low flow, flush, and declining flow. This classification was informed by temporal patterns in discharge and PDSI values, observed consistently across the four monitoring sites. Declining flow was characterized with the onset of dry conditions depicted by the PDSI turning negative. Low flow marks the phase when the flow remains at very low rates although the surface system has started to recover from the trying phase. Flush is defined by the onset of high discharge. The hydrological phases will be complemented with hysteresis phases later on.

### 2.6.2 Pollution Load Index

We further calculated the Pollution Load Index (PLI) to assess the cumulative level of metal(loid) contamination across the four flow monitored locations. The PLI provides an aggregated measure of contamination by integration the contamination factors (CFs) of individual metal(loid)s, calculated as a ratio of observed metal(loid) concentrations to their respective background reference values (Jahan and Strezov, 2018):

$$PLI = (CF_1 \times CF_2 \times CF_3 \dots \dots CF_n)^{1/n} \quad (1)$$

where  $CF = C_{\text{metal}}/C_{\text{background}}$ , and  $n$  is the number of metal(loid)s considered. A  $PLI > 1$  indicates pollution, whereas  $PLI < 1$  implies no contamination (Tomlinson et al., 1980). Reference concentrations (for all metal(loid)s except Al) were derived from average values in the Elbe river at the Magdeburg station, located near the midpoint of the river, for the year 2022, obtained from FGG Elbe Data Portal (Datenportal der FGG Elbe, 2025). This evaluation allowed us to assess relative contamination levels at specific locations in the mine against a representative background from a major regional river.

### 2.6.3 Concentration-Discharge analysis



Concentration-discharge (C-Q) relationships were analyzed in  $\log_{10}$ - $\log_{10}$  space to determine whether certain areas of the mine disproportionately contribute specific metal(loid)s across the hydrological phases. The slope (b) value of each C-Q relationship was used as the primary metric to evaluate site-specific solute behavior (Fig. 1). Flat or near-zero slopes indicate chemostatic conditions, where concentrations remain stable with varying discharge. Negative slopes reflect source-limited dilution, as solute sources become insufficient at higher flows (Basu et al., 2010). Positive slopes reflect enrichment, pointing to transport-limited mobilization driven by large solute stores and increased hydrological connectivity (Pohle et al., 2021).

#### 2.6.4 Hysteresis analysis

To capture dynamic transport mechanisms, hysteresis behavior in C-Q relationships was also evaluated using hysteresis index (HI) methods developed by Lloyd et al. (2016) and Zuecco et al. (2016). These approaches quantify the direction and magnitude of hysteresis loops observed across different phases. Clockwise hysteresis reflects higher concentrations on the rising limb, suggesting rapid mobilization and proximity of hydrogeochemical sources, whereas counterclockwise hysteresis occurs when concentrations on the falling limb exceed those on the rising limb, indicating that high concentration sources are distant from the sampling location (Pohle et al., 2021).

To compare across events, sites, and solutes, HI values were computed using normalized discharge and concentration values. The Lloyd et al. (2016) method defines HI as the difference in normalized C and Q between rising and falling limbs, while the Zuecco et al. (2016) method interprets the vector angle between these phases to infer transfer behavior. In both cases, HI values range from -1 to +1, with positive values indicating clockwise hysteresis and negative values indicating counterclockwise hysteresis (Vaughan et al., 2017). These indices enable systematic identification of shifts in contaminant availability, transport timing, and hydrogeochemical memory across the mine system.

#### 2.6.5 Hydrogeochemically defined phases

In addition to the hydrologically defined phases, we introduced geochemically defined phases to resolve finer-scale temporal variability in contaminant mobilization. The following phases and hysteresis classes were derived based on a point-to-point analysis of the C-Q patterns for each solute and site: Loading with  $Q \downarrow C \uparrow$ , flushing with  $Q \uparrow C \uparrow$ , dilution with  $Q \uparrow C \downarrow$ , chemostatic with varying Q and stable C, recession with  $Q \downarrow C \downarrow$  and variable sources with stable Q and varying C. The hysteresis phase classification was based on the direction of the C-Q loop as counter-clockwise (distant sources, delayed response) with negative HI and clockwise (near-stream sources, rapid mobilization) with positive HI. The points of maximum pollution potential were identified when high concentrations were reached in loading or flushing before transitioning to a substantial dilution.

Following this classification, the general pattern of a clockwise loading phase during declining and low flow followed by a substantial dilution can be found for the heavy metals. This event and site-specific phase framework provided a mechanistic understanding of solute mobilization pathways that complemented the broader hydrological regime.



## 305 2.6.6 Data visualization

All figures and data visualizations were produced using Python (v3.12), primarily with the pandas and plotly libraries, and are reproducible (see Sanchez et al., 2025b). The conceptual frameworks outlined in Fig.'s 1 and 2 further guided our analysis, motivating the structure of the results to follow the dynamics of flow-phase-dependent connectivity and site-specific contaminant mobilization.

## 310 3 Results and discussion

### 3.1 Spatial and temporal patterns in hydrological and geochemical parameters

The hydrological regime of the Reiche Zeche mine system exhibits pronounced temporal and spatial heterogeneity, driven by internal storage thresholds and episodic connectivity. Figure 3 summarizes key surface and subsurface hydrologic indicators, including the water availability index (PDSI), precipitation, and discharge at the four monitored sites. Based on hydro-  
315 meteorological observations, declining flow, low flow, and flush phases of the mine drainage dynamics were identified. The declining phase is informed by the overall moisture regime starting with the landscape shift from wet to dry states and ending when both flow and dryness reach their minimum. These patterns were exhibited for two annual cycles (i.e. in 2022 and 2023). Notably, flush phases occurred in February 2023 – May 2023 and December 2023 – February 2024, marked by sharp increases in discharge across all four sites. Discharge trends did not align tightly with precipitation inputs, suggesting delayed and non-  
320 linear hydrological responses (Milly et al., 2002; Bales et al., 2018). Although surface conditions transitioned from drought to wetter periods in early autumn, increased mine water discharge only became evident months later. This temporal disconnect likely reflects threshold-based fill-and-spill dynamics within vertically structured storage zones, where deeper sites (i.e., sites 3A and 3B) showing more pronounced discharge peaks than sites closer to the surface (Li et al., 2022) (i.e., site 1). These patterns imply that connectivity is not continuously active, but rather modulated by threshold exceedance, consistent with a  
325 fill-and-spill mechanism.

To further understand these patterns, we assessed spatial and temporal trends in the pollution load index (PLI) (Jahan and Strezov, 2018), which integrates multiple dissolved metal(loid) concentrations into a single risk metric (Fig. 3f). The PLI time series reveal clear site- and flow phase dependent variability. Notably, site 3A consistently exhibited the highest PLI values, often exceeding a value of 500, well above the pollution threshold of one (Tomlinson et al., 1980). These elevated PLI values  
330 declined sharply early in the flush events, consistent with dilution by low ionic strength water and enhanced mixing (Cánovas et al., 2007), and further suggesting solute buildup during low connectivity followed by rapid export when flow paths are reactivated.

We further classified the geochemical response at each site into distinct phases reflecting shifts in source zone activation and storage-release dynamics. These phases, derived from C-Q relationships and aligned with hydrologically defined flow  
335 conditions, include loading (characterized by solute accumulation during low flow), flushing (rapid contaminant release upon reactivation), dilution (declining concentrations with rising discharge), recession (post-flush declines in both flow and solute levels), and variable phases (mixed or unstable transport conditions). This phase-based framework, illustrated by using PLI



trajectories (Fig. 3e), offers a dynamic perspective on how internal thresholds and subsurface connectivity shifts modulate contaminant export, which is not in phase with the discharge dynamics. This approach challenges traditional drainage-based hypotheses by revealing that solute export is not a continuous seepage process, but rather a sequence of non-linear mobilization events tied to internal storage activation.

Site-specific patterns highlight important contrasts in system behavior. While the top-most site 1 exhibited muted responses with the lowest PLI values, suggesting this point to depict the water entry into the subsurface deposit structures, sites 2, 3A, and 3B exhibited stronger temporal variability, indicative of reactive source zones. In the lead-up to flushing events, elevated dissolved metal(loid) concentrations suggest slow leaching or desorption during storage-dominated phases (Pohle et al., 2021; Speir et al., 2024), while post-flush declines point to transient depletion of lotic pools. These sharp PLI fluctuations and synchronized concentration responses (Fig. S1) highlight the episodic nature of contaminant release and support the view that reconnecting flow paths mobilize previously isolated geochemical reservoirs.

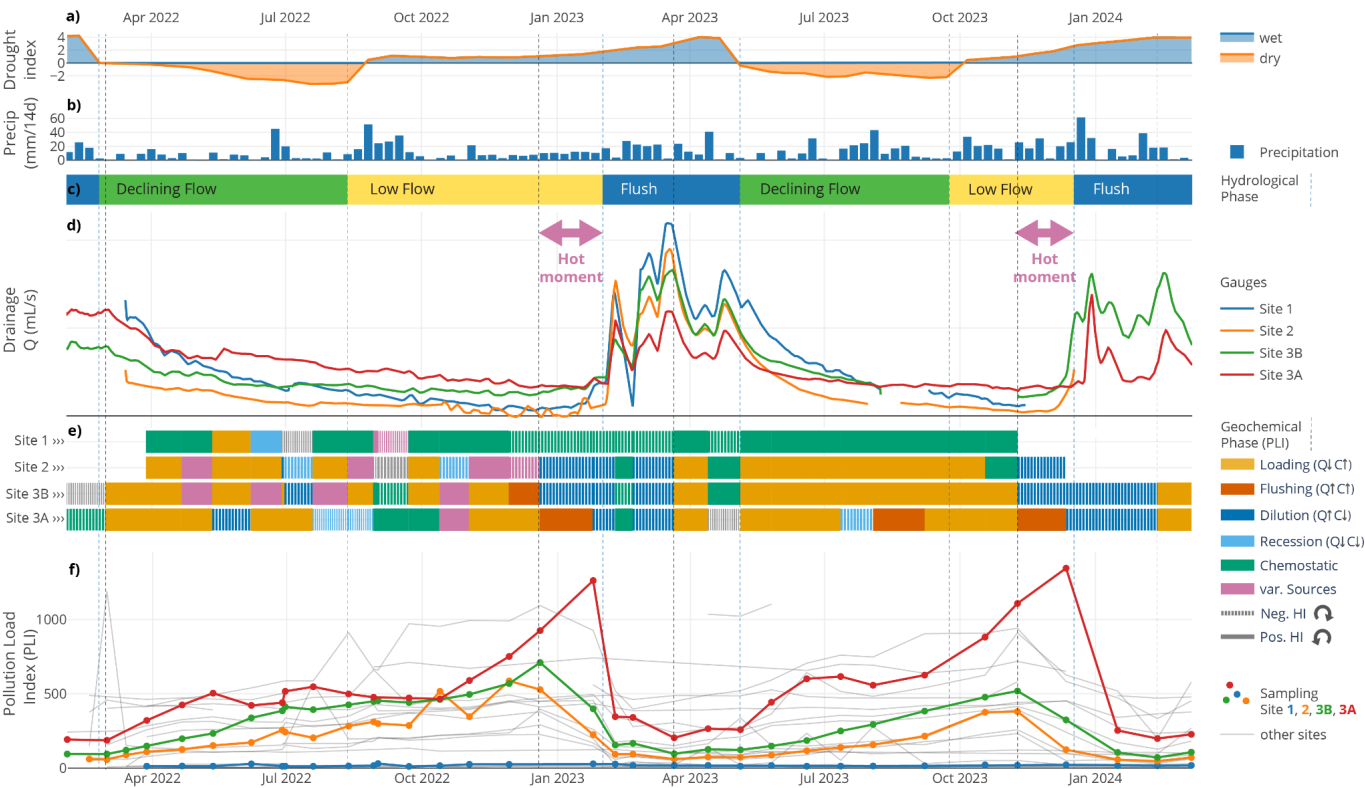


**Figure 3: Water and metal transport regime in the Reiche Zeche mine. (a)** Dryness index as an indicator of the general water situation on the surface. **(b)** Weekly precipitation collected from Reiche Zeche, Freiberg weather station. **(c)** Hydrologically defined flow phases. **(d)** Discharge at the four sites in the Reiche Zeche mine. Pink arrows represent time periods when hot moments occur. **(e)** Geochemical hysteresis phases of pollution load index (PLI) at the four sites. **(f)** PLI dynamics across the mine system. Grey area



355 reflects PLI values that are below the pollution threshold of 1. Individual sites are connected by black lines and colored lines are monitored flow sites for sites 1, 2, 3A, and 3B.

### 3.2 Trends in metal load patterns and isotopic deviations

While PLI values present a general overview of metal(loid) behavior, looking into metal specific dynamics revealed key insights into the mechanisms controlling contaminant release in legacy mine systems. The daily Zn load patterns observed at sites 3A and 3B (Fig. 4) exhibit sharp Zn load peaks shortly before major flushing events, despite relatively stable or declining discharge conditions. While these pre-flush peaks occurred during hydrologically low flow phases at both sites, the sites differ in terms of the contribution of each geochemical phase within their fill-and-spill dynamics, such that this is more pronounced for site 3A than site 3B. Once Zn accumulation is at its peak and mobilization begins, Zn loads drop abruptly, reflecting rapid dilution or depletion of accumulated pools. This suggests that site 3A may be a more important target for water remediation. Quantitatively, these short 2-3 month intervals account for 50-56% of the total annual Zn load at site 3A and 34-35% at site 3B, despite occupying less than 25% of the time period. This highlights a strong fill-and-spill style signature, where contaminants accumulate gradually under low connectivity and are then exported in intense but brief mobilization events. Importantly, the overlay of flow and geochemical phases emphasizes how metal mobilization is driven by the timing and sequence of hydrological reconnection.

To assess whether these mobilization pulses reflect deeper subsurface activation, we examined deviations in stable water isotope compositions ( $\delta^2\text{H}$  and  $\delta^{18}\text{O}$ ) between deeper sites (3A and 3B) and the shallower reference site 2 (Fig. 4c) as a measure of hydrologic connectivity. Individual samples plotted similarly close to the overall mine water background and the LMWL (Fig. S2), indicating only minor shifts in water sources and weathering interaction at this scale. However, large isotopic differences, predominantly during low flow periods in 2022, support the hypothesis of weak connectivity and more isolated subsurface storage compartments. These differences narrowed considerably during flush phases, indicating reactivation of previously disconnected zones. Shorter distances among standard deviations further point to site 3A (or 3B) being influenced by similar water sources as site 2 during flushing phases. These patterns extend prior applications of isotopic tracers beyond surface water systems (Spangenberg et al., 2007; Hazen et al., 2002), demonstrating their value for characterizing episodic hydrological activation and subsurface connectivity in mining environments.

These findings challenge the conventional focus on high-flow conditions as the primary drivers of contaminant export from mining-impacted systems. While prior studies have highlighted the role of high flow in resuspending contaminated sediments or altering water chemistry (e.g., via pH or redox shifts) (Hudson-Edwards et al., 1997; Dawson and Macklin, 1998), our results point to a dominant role of low flow inputs from subsurface or groundwater sources. Unlike classical baseflow, typically low in flow and constant in concentration, these low flow periods exhibited highly variable metal levels, indicating disproportionate contributions to contaminant loads from subsurface pools or intermittently connected sources. Similar conclusions have been drawn in other abandoned mine systems (Bryne et al., 2020), where metal fluxes were sustained or even



amplified under low flow regimes, underscoring the need to reconsider assumptions about contaminant risk during non-flushing conditions.

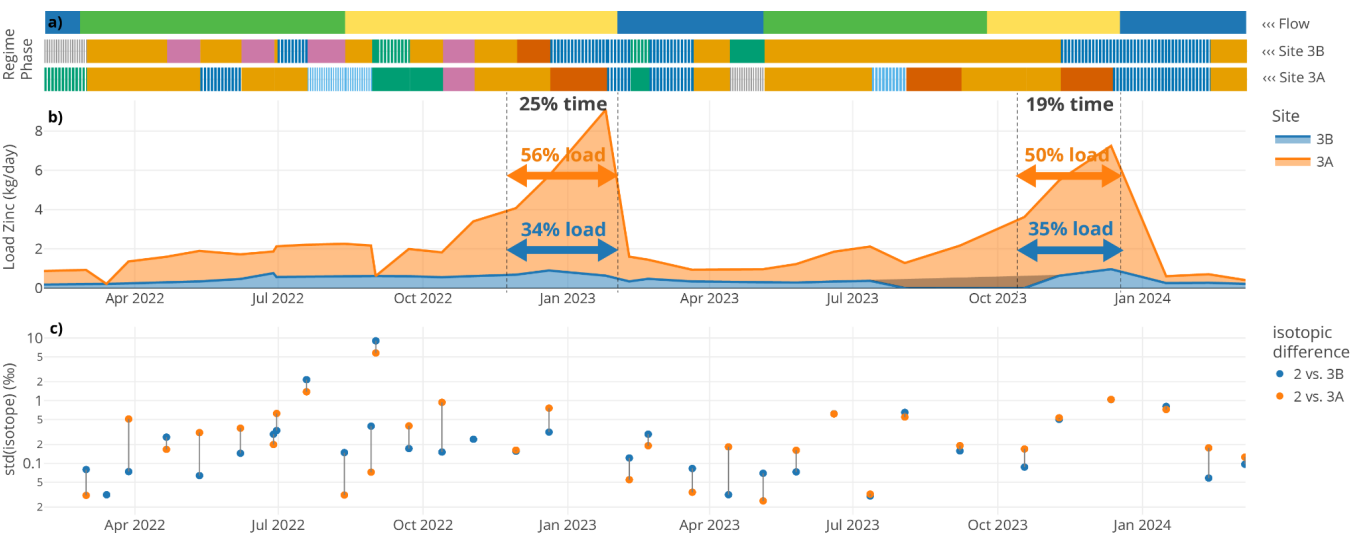


**Figure 4:** Zn loads and isotopic similarity from February 2022 to March 2024 are shown for sites 3A (orange) and 3B (blue). **a)** hydrological phases (declining: green, low: yellow, flush: blue) and corresponding geochemical phases (e.g., loading, flushing, recession, dilution, and variable) for sites 3A and 3B (as in Fig. 3). **b)** Zn loads with peak load contributions labeled as percentages, indicating the proportion of total Zn export occurring in the 2-3 months preceding flushing. Missing load values (shown in grey) between July and October 2023 for site 3B present periods where flow data was not obtained due to instrument error. **c)** Standard deviation of isotopic concentrations ( $\delta^{2}\text{H}$  and  $\delta^{18}\text{O}$ ) to site 2. Difference between 3A and 3B marked as vertical lines. The relative ratio marks how much the water is similar (strong connection in flow field) or distinct (disperse paths) in the drainage system.

The temporal synchronization of contaminant peaks across mine levels reveals a threshold-driven system governed by internal storage, episodic connectivity, and flow path structure. These processes collectively modulate metal(loid) transport and release, with site-specific patterns highlighting the role of delayed response and spatial heterogeneity in shaping contaminant export dynamics.

### 3.3 Dynamics in concentration-discharge relationships and hysteresis

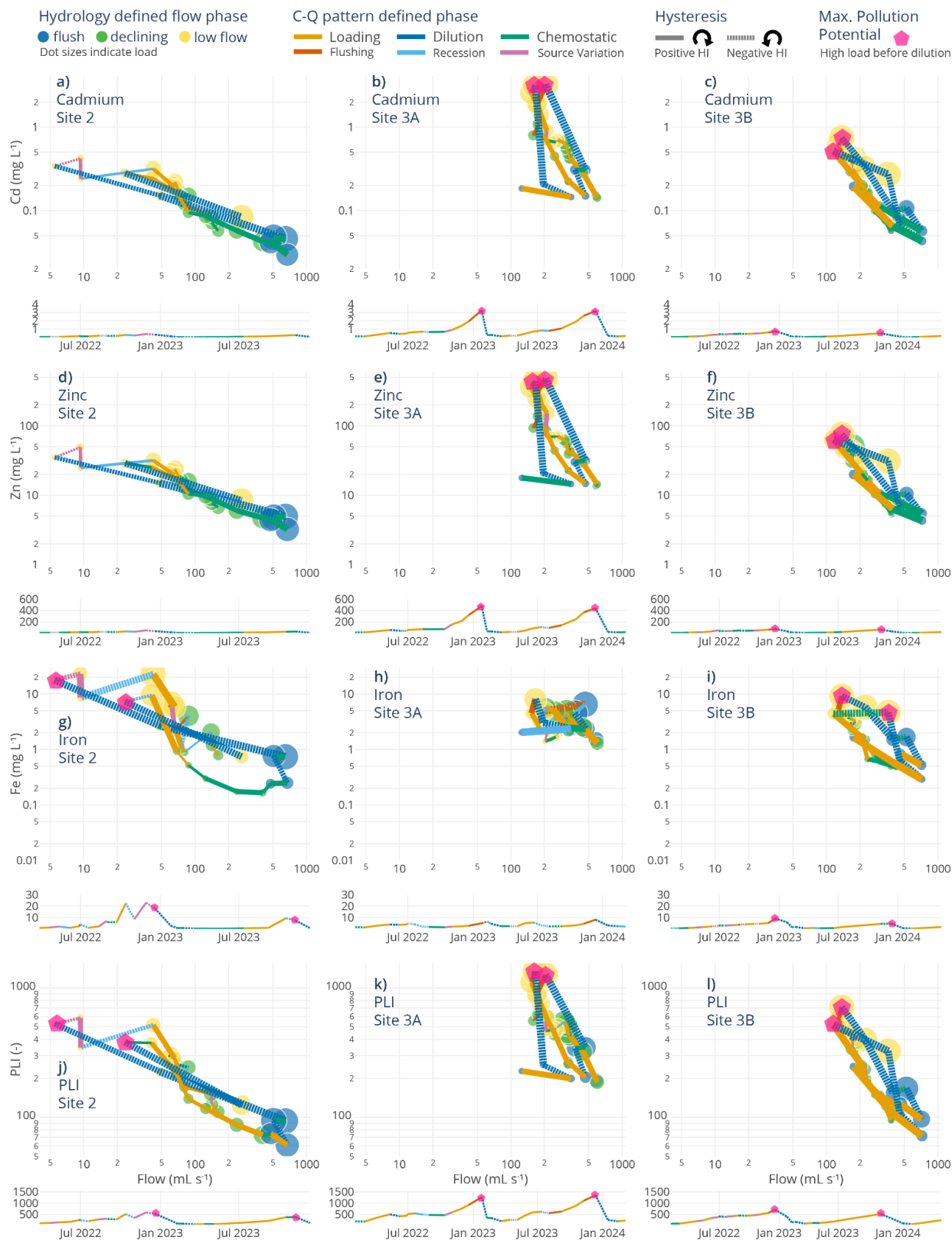
Going beyond temporal and spatial trends, C-Q slopes (Table S3) and hysteresis loops provide insight into solute source proximity, mobilization timing, and hydrological connectivity (Knapp et al., 2020). Figure 5 presents diagnostic C-Q relationships for Cd, Zn, Fe and PLI at sites 2, 3A, and 3B, integrating hydrologically and geochemically defined phases. C-Q slopes revealed very strong dilution patterns (slope  $< -1$ ) at sites 3A and 3B for Zn and Cd, in comparison to site 2 (slope = -0.55). This shift suggests a transition from proximal, source-limited mobilization at site 2 to more distal, transport-limited behavior at the deeper sites, where stored contaminants are more effectively diluted during high flow conditions.



Building on the phase-specific C-Q patterns, hysteresis index (HI) values, which quantify whether solute concentrations rise before or after peak flow, revealed reversals in solute transport dynamics across sites (Table S4). Pronounced hysteresis loops observed during low flow conditions preceding flushing events and HI values calculated using Lloyd et al. (2016) and Zuecco et al. (2016), supported asynchronous activation of flow paths. While we present the hysteresis loops using the method from Lloyd et al. (2016) in Fig. 5, both methods produced very similar results. Within these loops, we identified a “main pollution point”, the moment of peak concentration coinciding with minimal discharge, highlighting a critical window of contaminant risk. Eventually these points are followed by a shift to high flow and low concentration marked by dilution.

By averaging HI values from two methods (Lloyd et al., 2016; Zuecco et al., 2016), dissolved Cd and Zn displayed predominately counterclockwise hysteresis and dilution behavior during these main pollution point periods (e.g., at site 3A, Zn: HI = -1.05 and -0.78; Cd: HI = -1.03 and -0.81), suggesting delayed mobilization from deeper or disconnected zones (Speir et al., 2024). Dissolved Fe exhibited mixed hysteresis behavior, with counterclockwise hysteresis at site 3B (HI = -0.21 and -0.24) and near-zero hysteresis at site 3A, pointing to either complex or spatially uniform source zones (Rose et al., 2018; Zuecco et al., 2016). These patterns imply that individual metals respond differently to evolving hydrological or geochemical conditions, influenced by factors such as redox sensitivity, sorption behavior, and aqueous mobility (Galván et al., 2012).

PLI, which integrates all metal(loid) concentrations into a single risk index, showed similarly dynamic responses. The C-Q analysis revealed predominantly dilution behavior for all sites, but hysteresis was more specifically defined at sites 3A and 3B in comparison to site 2, suggesting a higher importance of observing mobilization transport in deeper areas of the mine after passage through legacy deposits of waste rock material. These site-specific differences underscore how the location, connectivity, and hydrodynamic activation of contaminant-rich zones govern release dynamics, highlighting that standard outlet-based monitoring may overlook episodic contributions from deeper, disconnected compartments. This has direct implications for the design of monitoring strategies and for timing interventions to capture or mitigate short-lived contaminant pulses.





435 **Figure 5: Concentration–discharge (C–Q) relationships ( $\log_{10}$  scaled) for (a–c) dissolved Cd, (d–f) dissolved Zn, (g–i) dissolved Fe, and (j–l) Pollution Load Index at Site 2 (a, d, g, j), Site 3A (b, e, h, k) and Site 3B (c, f, i, l) during the three hydrologically defined phases (flush - blue, declining - green, and low - yellow). Bright pink points are the main pollution points (i.e., moments within the low flow period when a hysteresis event was clearly observed). Dot size represents the respective load. Under each C–Q plot, the dissolved metal concentration and PLI values are shown across a time scale with bright pink symbols indicating when a hysteresis**  
440 **was identified from the C–Q plots. The geochemically defined phase from the C–Q patterns is represented through the color of the lines connecting each point for the C–Q plots with the line thickness corresponding to how large and fast the change in concentration and discharge is between the sampling points. This phase distinction is also shown for the time series with marked peak pollution points.**

445 The geochemically defined phases identified from these C–Q patterns reinforce these interpretations. During loading phases, elevated concentrations and rising discharge mark metal enrichment, while flushing phases show steep declines as flow paths reconnect. Dilution phases emerge when contaminant sources become depleted or overridden by clear inflows, frequently occurring when a main pollution point can be distinctly identified. The alignment of hysteresis moments with these geochemical transitions in the time-series subpanels underscores the threshold-driven and episodic nature of contaminant  
450 mobilization in this legacy mine system. These patterns highlight hysteresis direction and timing, rather than slope alone, are more diagnostic of changing flow path connectivity, source proximity, and depletion dynamics, consistent with fill-and-spill dynamics (Rose et al., 2018; Musolff et al., 2021).

### 3.4 Identification of high contaminant potential through spectrometric data

455 To complement this integrative view from the bi-weekly sampling and to zoom into the transition from loading to mobilization, we applied high-frequency monitoring with an in-situ UV-Vis spectrometer (collecting hourly measurements) and daily autosampling at site 2. At site 2, a drainage channel with rough bottom structure creates a specific dynamic flow environment where stratification, density contrasts, and throughflow coexisted (Sanchez et al., 2025). This setting created a labile 2-phase system: a low-density surface layer forming a hydraulically connected stream above a dense, metal-enriched bottom pool.  
460 Such dual compartments acted as both storage and release zones, with stratification intermittently buffering and then abruptly mobilizing contaminants. To capture these dynamics, we combined autosampler-based laboratory measurements with high-frequency spectrometric estimates of dissolved Cd (Fig. 6). This dual approach revealed that transitions from accumulation to flushing occurred within hours and much more rapid than what can be resolved by sampling alone, highlighting short-lived but significant windows of contaminant export.

465 All monitoring methods consistently showed Cd buildup during low and declining flow (July – December), followed by sharp concentration drops at the onset of flushing conditions. These shifts reinforce the role of threshold-based activation and transient hydrological connectivity in controlling solute mobilization. Notably, stratification observed visually in mid-October 2022 to late January revealed Cd concentrations in bottom grab samples (positioned near the channel base) more than two orders of magnitude higher than top grab samples (collected at the surface). The grey polygon (i.e., grab sample corridor) in



470 Fig. 6a delineates the concentration range captured by these paired depth-integrated manual grab samples, as well as the  
spectrolyzer results over the low flow period, providing a window into the presence of density-stabilized, solute-rich bottom  
waters. These findings suggest temporary solute traps forming during quiescent conditions, a phenomenon also reported in  
mine systems with intermediate density layering that can be rapidly flushed upon reactivation (Mugova and Wolkersdorfer,  
2022; Mugova and Wolkersdorfer, 2024).

475 Figure 6b illustrates how phase-specific C-Q relationships for dissolved Cd evolved during a six-week period leading up to  
the major flushing event in February 2023. Hourly data revealed shifting mobilization regimes, with clear transitions between  
chemostatic and chemodynamic behavior, just before hydrological shifts. Each C-Q panel corresponds to a high-resolution  
subwindow from the flow time series, capturing short-lived events with discrete geochemical responses. This highlights how  
although during small or intermediate increases in flow chemostatic conditions may prevail, in a short time span these  
480 conditions can change and be initiated from accumulated solute pools, especially under stratified or semi-stratified conditions  
where density-driven segregation creates temporary storage zones. During low to moderate flow conditions, even minor  
discharge increases can lead to the buildup prior to contaminant mobilization when residual sources remain available, eroding  
micro-stratification and reconnecting isolated pools with high pollution potential. In contrast, during high flow conditions,  
when temporary storages are already exhausted, these pools may be heavily mobilized, such that a variability of dilution,  
485 loading, and recession typically dominate the C-Q relationship (Fig. 6b, ‘Mobilization and eventual beginning of dilution’  
panel). Solute transport regimes transition within just a few days to weeks as discharge fluctuates, underscoring the dynamic  
connectivity of source zones and complements the broader patterns seen across sites and metals in Fig. 5. These findings  
reinforce that episodic hydrological forcing can lead to metal-specific, rapidly evolving export regimes that cannot be captured  
by temporal sampling alone.

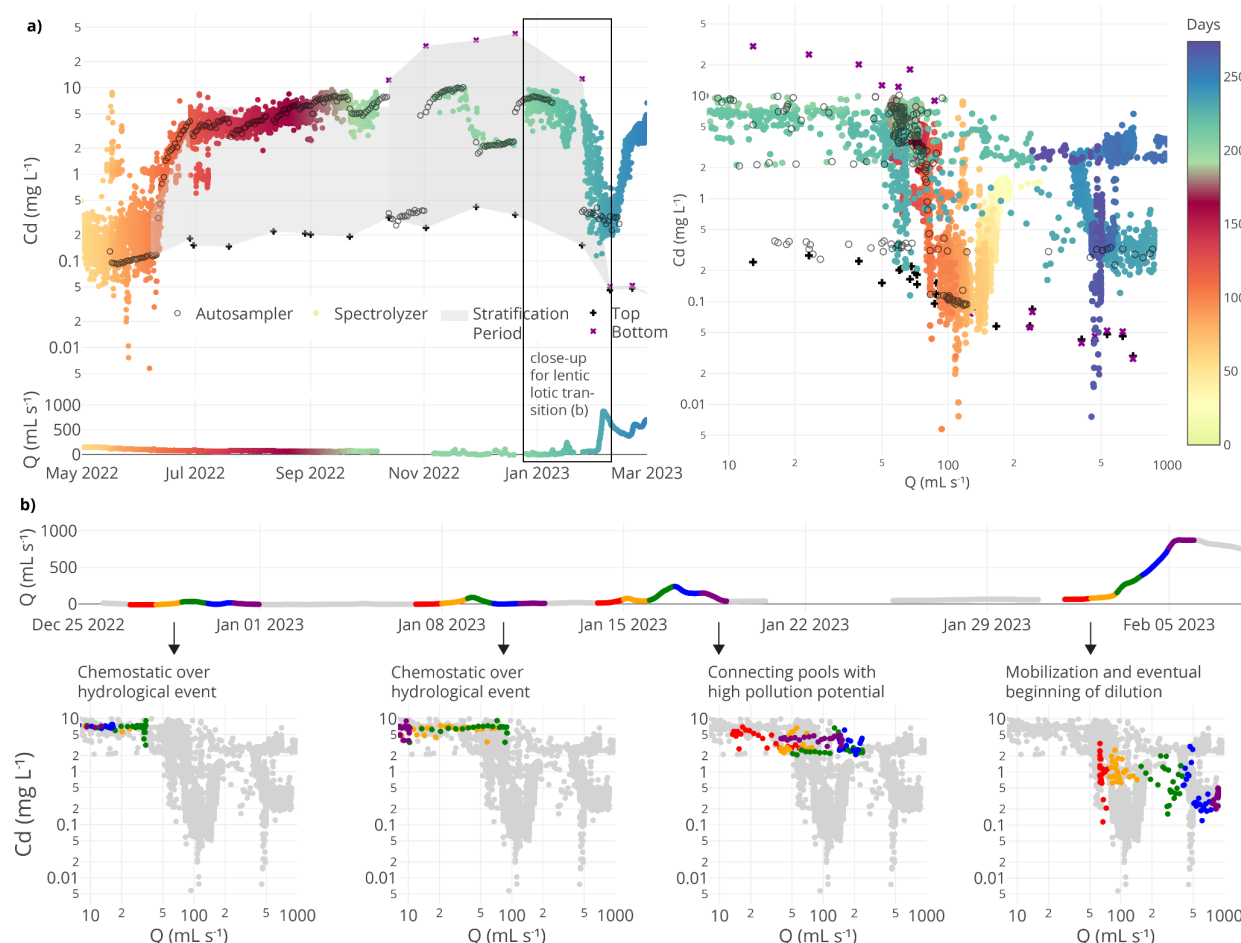


**Figure 6:** (a) Top right panel: Dissolved Cd concentrations ( $\log_{10}$  scaled) at site 2 measured using an autosampler (daily values in open circles), the spectrolyzer instrument (hourly values in colored circles), and manual sampling (bottom - purple crosses; top - black crosses). The grab sample corridor (grey polygon) represents the concentration range in which stratification was evident based on all sampling methods (until stratification collapse). The spectrolyzer measurements are colored by sampling day to indicate temporal regression. The black box with the annotation of close-up for lentic lotic transition highlights the six-week window analyzed in detail in panel b. Bottom panel: The time series for the water discharge matching with the spectrolyzer color scheme. Top left panel: C-Q relationship ( $\log_{10}$  scaled) for dissolved Cd following the same spectrolyzer color scheme as the right panel. (b) Top panel: The time series of the six-week window for the discharge matching with the spectrolyzer color scheme. Bottom panels: Phase-resolved C-Q patterns ( $\log_{10}$  scaled) for dissolved Cd over the stratification-collapse and lentic-lotic transition. Each small C-Q panel shows hourly Cd-Q data for a 5-day segment, with points colored by each day (day 1 - red, day 2 - orange, day 3 - green, day 4 - blue, day 5 - purple). C-Q plots highlight progressive phases in the transition between lentic to lotic or fill to spill conditions. After the first two hydrological events showing chemostatic characteristics (2022-12-27 to 2022-12-31 and 2023-01-07 to 2023-01-11), the third event hints to reconnecting pools with high pollution potential (2023-01-14 to 2023-01-18), which are eventually mobilized in



the fourth and strongest breakthrough event mobilization (2023-02-01 to 2023-02-05). These panels are linked to their respective periods in the hourly discharge time series.

The combined use of autosampler and high-frequency spectrolyzer data offer synergistic insights, such that the former anchors the dataset in analytical accuracy, while the latter captures transient solute behavior and enables time-resolved analysis of flow-phase transitions. This integrated perspective, alongside zooming into small time windows of C-Q responses, is critical for detecting and characterizing hot moments, in which brief but disproportionate pulses of metal export can dominate annual metal loads. Our findings emphasize that stratified pools stabilized during low flow can be rapidly activated within a short window during fill-and-spill (McDonnell et al., 2021) or lentic-lotic cycle transitions (Shaw et al., 2020), reinforcing the need for depth-aware, event-sensitive monitoring to anticipate episodic contaminant risks in complex mining systems.

### 3.5 Implications for contaminant pollution remediation

Our findings highlight that contaminant mobilization in abandoned mine systems is not primarily driven by storm intensity or seasonal high flows, but by internal hydrological thresholds and episodic connectivity between stored contaminant pools and the active drainage network. The observed lag between peak accumulation and flushing, followed by rapid load collapse, suggests that predictive assessments must incorporate not just hydrometeorological variables but also the internal memory of the system.

These dynamics expose critical blind spots in current water quality monitoring and regulatory frameworks. Existing benchmarks, such as German sediment quality guidelines (e.g., 800 mg/kg Zn in suspended materials) (Bundesamt für Justiz, 2016) and EU background dissolved Zn concentrations (1–35 µg/L) (Munn et al., 2010; Comber et al., 2008) overlook the timing and intensity of short-lived, high-risk release events from underground contaminant reservoirs. Figures 5 and 6 illustrate this clearly. Figure 5 provides a system-scale diagnostic, showing how metals and PLI evolve across sites and flow phases, with highlighted hot moments pinpointing pulses that carry disproportionate contaminant loads. Figure 6 then zooms in at high temporal resolution, capturing the collapse of stratification and lentic-lotic transition that triggered a breakthrough event. Therefore, the hot moments of release, which arise during hydrologically quiet intervals rather than extreme events, may represent important windows of strategic intervention.

While this study focuses on the Reiche Zeche mine, the fill-and-spill dynamics we observe are likely widespread across hydrologically complex, mining-impacted systems, especially in porous systems with variable subsurface connectivity, stratified drainage zones, or episodic flow regimes. Similar mechanisms may be active in karst aquifers, tunnel-fed drainages, or engineered infrastructure where discrete contaminant pools are intermittently connected to surface outflows. This shift from peak flow emphasis in such systems toward detecting internal system thresholds supports a more proactive, precise, and strategic path for better timed remediation. Effective mitigation depends on anticipating these moments before widespread flushing, when contaminant concentrations are high but spatially contained.



At site 3A, located near the central drainage adit and consistently exhibiting the highest PLI values, we observed Zn loads up to 8.4 kg/day prior to a major flush event (mean 1.9 kg/day). This site contributes only 0.06% of the overall water to the outlet of the overall adit Rothschnberger Stolln, but 1.3% of the Zn load in average (LfULG, 2014) with the few days before flushing accounting for about 50% of the annual load. This comparison underscores that substantial contaminant fluxes can accumulate and be released from within the mine system itself, often remaining undetected by conventional downstream monitoring. By combining C-Q relationships and hysteresis analysis, our approach pinpoints internal hotspots and identifies hot moments of high mobilization risk, advancing a framework to guide targeted monitoring and early-warning systems. Beyond this study, these findings highlight the broader relevance of upstream diagnostics for understanding contaminant behavior in legacy mine settings and support the need for spatially resolved, phase-sensitive strategies for remediation planning. The latter could include specific small-scale treatment systems near to the actual mobilization hotspots in the legacy mines.

#### 4 Conclusions

This study demonstrates that contaminant mobilization in abandoned mine systems is controlled not by steady seepage but by episodic shifts in internal hydrological connectivity. Across the Reiche Zeche mine, low flow and pre-flush phases were shown to concentrate dissolved metal(loid)s in poorly connected storage zones, with subsequent reconnection triggering sharp but short-lived contaminant releases. Event-scale C-Q relationships and hysteresis patterns reveal that such hot moments of export account for a disproportionate share of annual metal loads, emphasizing the need to move beyond traditional outlet-based monitoring. Our findings highlight three key insights. First, low flow periods represent high risk intervals of solute accumulation, challenging assumptions that contaminant risk is greatest only during floods or peak flows. Second, site-specific patterns demonstrate that deeper, variably connected zones dominate contaminant export dynamics, underscoring the importance of subsurface heterogeneity. Third, targeted monitoring of connectivity threshold provides a basis for early warning and site-specific and near-source interventions. By identifying internal hotspots and the timing of mobilization events, this work establishes a transferable framework for diagnosing contaminant risks in legacy mine settings. These insights support a shift toward event-sensitive, near-source remediation strategies that prioritize internal system dynamics, offering more efficient and scalable alternatives to conventional end-of-pipe treatment.

#### Author contributions

**Anita Alexandra Sanchez:** Conceptualization, Methodology, Formal analysis, Investigation, Data curation, Writing-original draft, Writing-review and editing. **Maximilian P. Lau:** Conceptualization, Supervision, Validation, Writing: review and editing. **Sean Adam:** Spectral data analysis, online UV-Vis Spectrometer data curation. **Sabrina Hedrich:** Validation, Writing: review and editing. **Conrad Jackisch:** Conceptualization, Supervision, Hydrological and hysteresis analysis, Data visualization and curation, Original Writing-original draft, Writing: review and editing.

#### 570 Data Availability Statement



The dataset supporting this study is openly available via the B2SHARE data repository under the title LegacyMine\_HydroGeo: Dataset on the geochemical and hydrological dynamics in a historic mine system (Sanchez et al., 2025b). It includes high-resolution geochemical, isotopic, hydrological, and spectrometric data collected from the Reiche Zeche mine over a two-year monitoring period. The dataset can be accessed at <https://doi.org/10.23728/b2share.32958b4c93284b739182774a18756fdb>.

575

### Competing interests

The authors declare that they have no conflict of interest.

### Acknowledgements

580 This research was conducted as part of the project "Source Related Control and Treatment of Saxon Mining Water" and was funded by the Dr. Erich-Krüger Foundation. We extend our gratitude to Dr. Alexander Pleßow for his support with laboratory equipment. Special thanks to Prof. Helmut Mischo and Stephan Leibelt for their training and access to the Reiche Zeche mine, as well as to Dr. Andreas Kluge and Dr. Nils Hoth for their invaluable assistance in initiating work on the mine system. We also wish to acknowledge the laboratory team—Thurit Tschöpe, Marius Stoll, Claudia Malz, Eva Fischer, and Lena Grundmann—for their help with sample measurements, as well as Karl Haas and Lena Herzig for her assistance in collecting mine water samples.

585

### References

- Allen, D. M. and Voormeij, D. A.: Oxygen-18 and Deuterium Fingerprinting of Tailings Seepage at the Sullivan Mine, Mine Water Environ., 21, 168–182, <https://doi.org/10.1007/s102300200041>, 2002.
- 590 Balerna, J. A., Melone, J. C., and Knee, K. L.: Using concentration-discharge relationships to identify influences on surface and subsurface water chemistry along a watershed urbanization gradient, Water (Switzerland), 13, <https://doi.org/10.3390/w13050662>, 2021.
- 595 Bales, R. C., Goulden, M. L., Hunsaker, C. T., Conklin, M. H., Hartsough, P. C., O’Geen, A. T., Hopmans, J. W., and Safeeq, M.: Mechanisms controlling the impact of multi-year drought on mountain hydrology, Sci. Rep., 8, 690, <https://doi.org/10.1038/s41598-017-19007-0>, 2018.
- 600 Basu, N. B., Destouni, G., Jawitz, J. W., Thompson, S. E., Loukinova, N. V., Darracq, A., Zanardo, S., Yaeger, M., Sivapalan, M., Rinaldo, A., and Rao, P. S. C.: Nutrient loads exported from managed catchments reveal emergent biogeochemical stationarity, Geophys. Res. Lett., 37, <https://doi.org/10.1029/2010gl045168>, 2010.
- Bozau, E., Licha, T., and Ließmann, W.: Hydrogeochemical characteristics of mine water in the Harz Mountains, Germany, Chemie der Erde, 77, 614–624, <https://doi.org/10.1016/j.chemer.2017.10.001>, 2017.
- 605 Bundesamt für Justiz – Verordnung zum Schutz der Oberflächengewässer 1 Anlage 6: [https://www.gesetze-im-internet.de/ogewv\\_2016/anlage\\_6.html](https://www.gesetze-im-internet.de/ogewv_2016/anlage_6.html), last access: 30 July 2025.



- 610 Burt, E. I., Allen, S. T., Braun, S., Tresch, S., Kirchner, J. W., and Goldsmith, G. R.: New Precipitation Is Scarce in Deep  
Soils: Findings From 47 Forest Plots Spanning Switzerland, *Geophys. Res. Lett.*, 52, <https://doi.org/10.1029/2025gl115274>,  
2025.
- 615 Byrne, P., Onnis, P., Runkel, R. L., Frau, I., Lynch, S. F. L., and Edwards, P.: Critical Shifts in Trace Metal Transport and  
Remediation Performance under Future Low River Flows, *Environ. Sci. Technol.*, 54, 15742–15750,  
<https://doi.org/10.1021/acs.est.0c04016>, 2020.
- Byrne, P., Wood, P. J., and Reid, I.: The Impairment of River Systems by Metal Mine Contamination: A Review Including  
Remediation Options, *Crit. Rev. Environ. Sci. Technol.*, 42, 2017–2077, <https://doi.org/10.1080/10643389.2011.574103>,  
620 2012.
- Cánovas, C. R., Olías, M., Nieto, J. M., Sarmiento, A. M., and Cerón, J. C.: Hydrogeochemical characteristics of the Tinto and  
Odiel Rivers (SW Spain). Factors controlling metal contents, *Sci. Total Environ.*, 373, 363–382,  
<https://doi.org/10.1016/j.scitotenv.2006.11.022>, 2007.
- 625 Clark, I. and Fritz, P. (1st Ed.): *Environmental Isotopes in Hydrogeology*, Lewis Publishers, New York, 342 pp., ISBN  
9780429069574, 1997.
- Comber, S. D. W., Merrington, G., Sturdy, L., Delbeke, K., and Assche, F. van: Copper and zinc water quality standards under  
630 the EU Water Framework Directive: The use of a tiered approach to estimate the levels of failure, *Sci. Total Environ.*, 403,  
12–22, <https://doi.org/10.1016/j.scitotenv.2008.05.017>, 2008.
- Datenportal der FGG Elbe: [https://elbe-datenportal.de/FisFggElbe/content/auswertung/MessstellenDetail\\_erstStart](https://elbe-datenportal.de/FisFggElbe/content/auswertung/MessstellenDetail_erstStart), last  
635 access: 11 July 2025.
- Datta, B., Durand, F., Laforge, S., Prakash, O., Esfahani, H. K., Chadalavada, S., and Naidu, R.: Preliminary Hydrogeologic  
Modeling and Optimal Monitoring Network Design for a Contaminated Abandoned Mine Site Area: Application of Developed  
Monitoring Network Design Software, *J. Water Resour. Prot.*, 08, 46–64, <https://doi.org/10.4236/jwarp.2016.81005>, 2016.
- 640 Dawson, E. J. and Macklin, M. G.: Speciation of heavy metals on suspended sediment under high flow conditions in the River  
Aire, West Yorkshire, UK, *Hydrol. Process.*, 12, 1483–1494, [https://doi.org/10.1002/\(sici\)1099-1085\(199807\)12:9<1483::aid-  
hyp651>3.0.co;2-w](https://doi.org/10.1002/(sici)1099-1085(199807)12:9<1483::aid-hyp651>3.0.co;2-w), 1998.
- Fovet, O., Belemtougri, A., Boithias, L., Braud, I., Charlier, J., Cottet, M., Daudin, K., Dramais, G., Ducharne, A., Folton, N.,  
645 Grippa, M., Hector, B., Kuppel, S., Coz, J. L., Legal, L., Martin, P., Moatar, F., Molénat, J., Probst, A., Riotte, J., Vidal, J.,  
Vinatier, F., and Datry, T.: Intermittent rivers and ephemeral streams: Perspectives for critical zone science and research on  
socio-ecosystems, *Wiley Interdiscip. Rev.: Water*, 8, <https://doi.org/10.1002/wat2.1523>, 2021.
- Freeman, M. C., Pringle, C. M., and Jackson, C. R.: Hydrologic Connectivity and the Contribution of Stream Headwaters to  
650 Ecological Integrity at Regional Scales<sup>1</sup>, *JAWRA J. Am. Water Resour. Assoc.*, 43, 5–14, [https://doi.org/10.1111/j.1752-  
1688.2007.00002.x](https://doi.org/10.1111/j.1752-1688.2007.00002.x), 2007.
- Galván, L., Olías, M., Cánovas, C. R., Torres, E., Ayora, C., Nieto, J. M., and Sarmiento, A. M.: Refining the estimation of  
metal loads dissolved in acid mine drainage by continuous monitoring of specific conductivity and water level, *Applied  
Geochemistry*, 27, 1932–1943, <https://doi.org/10.1016/j.apgeochem.2012.07.011>, 2012.
- 655 Ghomshei, M. M. and Allen, D. M.: *Potential application of oxygen-18 and deuterium in mining effluent and acid rock drainage  
studies*, Springer-Verlag, 2000.



- 660 Godsey, S. E., Kirchner, J. W., and Clow, D. W.: Concentration-discharge relationships reflect chemostatic characteristics of US catchments, *Hydrological Processes*, 23, 1844–1864, <https://doi.org/10.1002/hyp.7315>, 2009.
- Haferburg, G., Krichler, T., and Hedrich, S.: Prokaryotic communities in the historic silver mine Reiche Zeche, *Extremophiles*, 26, <https://doi.org/10.1007/s00792-021-01249-6>, 2022.
- 665 Hazen, J. M., Williams, M. W., Stover, B., and Wireman, M.: Characterisation of Acid Mine Drainage Using a Combination of Hydrometric, Chemical and Isotopic Analyses, Mary Murphy Mine, Colorado, 2002.
- Henderson, F. M.: *Open Channel Flow*, MacMillan, New York, 1966.
- 670 Herndon, E. M., Dere, A. L., Sullivan, P. L., Norris, D., Reynolds, B., and Brantley, S. L.: Landscape heterogeneity drives contrasting concentration-discharge relationships in shale headwater catchments, *Hydrology and Earth System Sciences*, 19, 3333–3347, <https://doi.org/10.5194/hess-19-3333-2015>, 2015.
- 675 Huang, C., Guo, Z., Li, T., Xu, R., Peng, C., Gao, Z., and Zhong, L.: Source identification and migration fate of metal(loid)s in soil and groundwater from an abandoned Pb/Zn mine, *Science of the Total Environment*, 895, <https://doi.org/10.1016/j.scitotenv.2023.165037>, 2023.
- 680 Hudson, E., Kulassa, B., Edwards, P., Williams, T., and Walsh, R.: Integrated Hydrological and Geophysical Characterisation of Surface and Subsurface Water Contamination at Abandoned Metal Mines, *Water, Air, Soil Pollut.*, 229, 256, <https://doi.org/10.1007/s11270-018-3880-4>, 2018.
- Hudson-Edwards, K., Macklin, M., and Taylor, M.: Historic metal mining inputs to Tees river sediment, *Sci. Total Environ.*, 194, 437–445, [https://doi.org/10.1016/s0048-9697\(96\)05381-8](https://doi.org/10.1016/s0048-9697(96)05381-8), 1997.
- 685 Jahan, S. and Strezov, V.: Comparison of pollution indices for the assessment of heavy metals in the sediments of seaports of NSW, Australia, *Mar. Pollut. Bull.*, 128, 295–306, <https://doi.org/10.1016/j.marpolbul.2018.01.036>, 2018.
- 690 Kimball, B. A., Runkel, R. L., Walton-Day, K., and Bencala, K. E.: Assessment of metal loads in watersheds affected by acid mine drainage by using tracer injection and synoptic sampling: Cement Creek, Colorado, USA, *Applied Geochemistry*, 17, 1183–1207, [https://doi.org/10.1016/s0883-2927\(02\)00017-3](https://doi.org/10.1016/s0883-2927(02)00017-3), 2002.
- Knapp, J. L. A., Freyberg, J. von, Studer, B., Kiewiet, L., and Kirchner, J. W.: Concentration–discharge relationships vary among hydrological events, reflecting differences in event characteristics, *Hydrol. Earth Syst. Sci.*, 24, 2561–2576, <https://doi.org/10.5194/hess-24-2561-2020>, 2020.
- 695 Kuhn, M., and Johnson, K. (1st Ed.): *Applied Predictive Modeling*, Springer, New York, 600 pp., ISBN 978-1-4614-6849-3, 2013.
- 700 Kumar, V., Paul, D., and Kumar, S.: Acid mine drainage from coal mines in the eastern Himalayan sub-region: Hydrogeochemical processes, seasonal variations and insights from hydrogen and oxygen stable isotopes, *Environ. Res.*, 252, 119086, <https://doi.org/10.1016/j.envres.2024.119086>, 2024.
- 705 Länderarbeitsgemeinschaft Wasser (LAWA): Arbeitshilfe zur Umsetzung der EG-Wasserrahmenrichtlinie, [https://www.lawa.de/documents/arbeitshilfe\\_30-04-2003\\_1552293505.pdf](https://www.lawa.de/documents/arbeitshilfe_30-04-2003_1552293505.pdf), 2003.
- Lemenkova, P.: Evaluating the Performance of Palmer Drought Severity Index (PDSI) in Various Vegetation Regions of the Ethiopian Highlands, *Acta Biologica Marisiensis*, 2021, 14–31, <https://doi.org/10.2478/abmj-2021-0010>, n.d.



- 710 Li, L., Bao, C., Sullivan, P. L., Brantley, S., Shi, Y., and Duffy, C.: Understanding watershed hydrogeochemistry: 2. Synchronized hydrological and geochemical processes drive stream chemostatic behavior, *Water Resour. Res.*, 53, 2346–2367, <https://doi.org/10.1002/2016wr018935>, 2017.
- 715 Li, Q., Ma, L., and Liu, T.: Transformation among precipitation, surface water, groundwater, and mine water in the Hailiutu River Basin under mining activity, *Journal of Arid Land*, 14, 620–636, <https://doi.org/10.1007/s40333-022-0020-1>, 2022.
- Liu, G., Xue, W., Tao, L., Liu, X., Hou, J., Wilton, M., Gao, D., Wang, A., and Li, R.: Vertical distribution and mobility of heavy metals in agricultural soils along Jishui River affected by mining in Jiangxi Province, China, *Clean - Soil, Air, Water*, 42, 1450–1456, <https://doi.org/10.1002/clen.201300668>, 2014.
- 720 Lloyd, C. E. M., Freer, J. E., Johnes, P. J., and Collins, A. L.: Technical Note: Testing an improved index for analysing storm discharge–concentration hysteresis, *Hydrol. Earth Syst. Sci.*, 20, 625–632, <https://doi.org/10.5194/hess-20-625-2016>, 2016.
- 725 Macklin, M. G., Thomas, C. J., Mudbhalkar, A., Brewer, P. A., Hudson-Edwards, K. A., Lewin, J., Scussolini, P., Eilander, D., Lechner, A., Owen, J., Bird, G., Kemp, D., and Mangalaa, K. R.: Impacts of metal mining on river systems: a global assessment, *Science*, 381, 1345–1350, <https://doi.org/10.1126/science.adg6704>, 2023.
- McDonnell, J. J., Spence, C., Karran, D. J., Meerveld, H. J. van, and Harman, C. J.: Fill-and-Spill: A Process Description of Runoff Generation at the Scale of the Beholder, *Water Resources Research*, 57, <https://doi.org/10.1029/2020wr027514>, 2021.
- 730 Merritt, P. and Power, C.: Assessing the long-term evolution of mine water quality in abandoned underground mine workings using first-flush based models, *Science of the Total Environment*, 846, <https://doi.org/10.1016/j.scitotenv.2022.157390>, 2022.
- 735 Milly, P. C. D., Wetherald, R. T., Dunne, K. A., and Delworth, T. L.: Increasing risk of great floods in a changing climate, *Nature*, 415, 514–517, <https://doi.org/10.1038/415514a>, 2002.
- Mischo, U.-P. D.-I. H., Eng, P., Barakos, D.-I. G., Szkliniarz, K., and Kisiel, J.: SITE DESCRIPTION AND DATA OF THE Reiche Zeche Site services, Characteristics and Data, 2021.
- 740 Mugova, E. and Wolkersdorfer, C.: Density stratification and double-diffusive convection in mine pools of flooded underground mines – A review, *Water Research*, 214, <https://doi.org/10.1016/j.watres.2021.118033>, 2022.
- Mugova, E., Molaba, L., and Wolkersdorfer, C.: Understanding the Mechanisms and Implications of the First Flush in Mine Pools: Insights from Field Studies in Europe’s Deepest Metal Mine and Analogue Modelling, *Mine Water Environ.*, 43, 73–86, <https://doi.org/10.1007/s10230-024-00969-3>, 2024.
- 745 Munn, S., Aschberger, K., Olsson, H., Pakalin, S., Pellegrini, G., Vegro, S., and Paya Perez, A.: European Union Risk Assessment Report - Zinc Metal. Publications Office of the European Union, Luxembourg, ISBN 978-92-79-17540-4, 2010.
- 750 Musolff, A., Fleckenstein, J. H., Rao, P. S. C., and Jawitz, J. W.: Emergent archetype patterns of coupled hydrologic and biogeochemical responses in catchments, *Geophysical Research Letters*, 44, 4143–4151, <https://doi.org/10.1002/2017gl072630>, 2017.
- 755 Musolff, A., Zhan, Q., Dupas, R., Minaudo, C., Fleckenstein, J. H., Rode, M., Dehaspe, J., and Rinke, K.: Spatial and Temporal Variability in Concentration-Discharge Relationships at the Event Scale, *Water Resour. Res.*, 57, <https://doi.org/10.1029/2020wr029442>, 2021.



- Palmer, S. M., Evans, C. D., Chapman, P. J., Burden, A., Jones, T. G., Allott, T. E. H., Evans, M. G., Moody, C. S., Worrall, F., and Holden, J.: Sporadic hotspots for physico-chemical retention of aquatic organic carbon: from peatland headwater source to sea, *Aquat. Sci.*, 78, 491–504, <https://doi.org/10.1007/s00027-015-0448-x>, 2016.
- Pohle, I., Baggaley, N., Palarea-Albaladejo, J., Stutter, M., and Glendell, M.: A Framework for Assessing Concentration-Discharge Catchment Behavior From Low-Frequency Water Quality Data, *Water Resources Research*, 57, <https://doi.org/10.1029/2021wr029692>, 2021.
- Resongles, E., Casiot, C., Freydier, R., Gall, M. L., and Elbaz-Poulichet, F.: Variation of dissolved and particulate metal(loid) (As, Cd, Pb, Sb, Tl, Zn) concentrations under varying discharge during a Mediterranean flood in a former mining watershed, the Gardon River (France), *Journal of Geochemical Exploration*, 158, <https://doi.org/10.1016/j.gexplo.2015.07.010>, 2015.
- Rose, L. A., Karwan, D. L., and Godsey, S. E.: Concentration–discharge relationships describe solute and sediment mobilization, reaction, and transport at event and longer timescales, *Hydrological Processes*, 32, 2829–2844, <https://doi.org/10.1002/hyp.13235>, 2018.
- Sächsisches Landesamt für Umwelt, Landwirtschaft und Geologie (LfULG): <https://lfulg.sachsen.de/>, last access: 11 July 2025.
- Sanchez, A. A., Haas, K., Jackisch, C., Hedrich, S., and Lau, M. P.: Enrichment of dissolved metal(loid)s and microbial organic matter during transit of a historic mine drainage system, *Water Res.*, 266, 122336, <https://doi.org/10.1016/j.watres.2024.122336>, 2024.
- Sanchez, A., Jackisch, C., Oelschlägel, M., Hedrich, S., and Lau, M. P.: Harmful metal export from abandoned mines controlled by hydrodynamic and biogeochemical drivers. *ACS ES&T Water. Article ASAP*, <https://10.1021/acsestwater.5c00334>, 2025.
- Sanchez, A. A., Lau, M. P., Adam, S. P., Haas, K. J., Hedrich, S., and Jackisch, C.: LegacyMine\_HydroGeo: Dataset on geochemical and hydrological dynamics in a historic mine system [Data set]. <https://b2share.eudat.eu>. <https://doi.org/10.23728/B2SHARE.32958B4C93284B739182774A18756FDB>, 2025b.
- Schmadel, N. M., Harvey, J. W., Alexander, R. B., Schwarz, G. E., Moore, R. B., Eng, K., Gomez-Velez, J. D., Boyer, E. W., and Scott, D.: Thresholds of lake and reservoir connectivity in river networks control nitrogen removal, *Nat. Commun.*, 9, 2779, <https://doi.org/10.1038/s41467-018-05156-x>, 2018.
- Sergeant, C. J., Sexton, E. K., Moore, J. W., Westwood, A. R., Nagorski, S. A., Ebersole, J. L., Chambers, D. M., O’Neal, S. L., Malison, R. L., Hauer, F. R., Whited, D. C., Weitz, J., Caldwell, J., Capito, M., Connor, M., Frissell, C. A., Knox, G., Lowery, E. D., Macnair, R., Marlatt, V., McIntyre, J. K., McPhee, M. V., and Skuce, N.: Risks of mining to salmonid-bearing watersheds, *Sci. Adv.*, 8, eabn0929, <https://doi.org/10.1126/sciadv.abn0929>, 2022.
- Shaw, M., Yazbek, L., Singer, D., and Herndon, E.: Seasonal mixing from intermittent flow drives concentration-discharge behaviour in a stream affected by coal mine drainage, *Hydrological Processes*, 34, 3669–3682, <https://doi.org/10.1002/hyp.13822>, 2020.
- Spangenberg, J. E., Dold, B., Vogt, M. L., and Pfeifer, H. R.: Stable hydrogen and oxygen isotope composition of waters from mine tailings in different climatic environments, *Environmental Science and Technology*, 41, 1870–1876, <https://doi.org/10.1021/es061654w>, 2007.



- Speir, S. L., Rose, L. A., Blaszcak, J. R., Kincaid, D. W., Fazekas, H. M., Webster, A. J., Wolford, M. A., Shogren, A. J., and Wymore, A. S.: Catchment concentration–discharge relationships across temporal scales: A review, *Wiley Interdiscip. Rev.: Water*, 11, <https://doi.org/10.1002/wat2.1702>, 2024.
- 810 Sprenger, M., Leistert, H., Gimbel, K., and Weiler, M.: Illuminating hydrological processes at the soil-vegetation-atmosphere interface with water stable isotopes, *Reviews of Geophysics*, 54, 674–704, <https://doi.org/10.1002/2015rg000515>, 2016.
- Turnbull, L., Hütt, M.-T., Ioannides, A. A., Kininmonth, S., Poepl, R., Tockner, K., Bracken, L. J., Keesstra, S., Liu, L., Masselink, R., and Parsons, A. J.: Connectivity and complex systems: learning from a multi-disciplinary perspective, *Appl. Netw. Sci.*, 3, 11, <https://doi.org/10.1007/s41109-018-0067-2>, 2018.
- 815 Tomlinson, D. L., Wilson, J. G., Harris, C. R., and Jeffrey, D. W.: Problems in the assessment of heavy-metal levels in estuaries and the formation of a pollution index, *Helgoländer Meeresunters.*, 33, 566–575, <https://doi.org/10.1007/bf02414780>, 1980.
- Vaughan, M. C. H., Bowden, W. B., Shanley, J. B., Vermilyea, A., Sleeper, R., Gold, A. J., Pradhanang, S. M., Inamdar, S. P., Levia, D. F., Andres, A. S., Birgand, F., and Schroth, A. W.: High-frequency dissolved organic carbon and nitrate measurements reveal differences in storm hysteresis and loading in relation to land cover and seasonality, *Water Resources Research*, 53, 5345–5363, <https://doi.org/10.1002/2017wr020491>, 2017.
- 820 Vidon, P., Allan, C., Burns, D., Duval, T. P., Gurwick, N., Inamdar, S., Lowrance, R., Okay, J., Scott, D., and Sebestyen, S.: Hot Spots and Hot Moments in Riparian Zones: Potential for Improved Water Quality Management, *JAWRA J. Am. Water Resour. Assoc.*, 46, 278–298, <https://doi.org/10.1111/j.1752-1688.2010.00420.x>, 2010.
- Wells, N., Goddard, S., and Hayes, M. J.: A Self-Calibrating Palmer Drought Severity Index, *J. Clim.*, 17, 2335–2351, [https://doi.org/10.1175/1520-0442\(2004\)017<2335:aspsi>2.0.co;2](https://doi.org/10.1175/1520-0442(2004)017<2335:aspsi>2.0.co;2), 2004.
- 830 Wilson, S. R., Hoyle, J., Measures, R., Ciacca, A. D., Morgan, L. K., Banks, E. W., Robb, L., and Wöhling, T.: Conceptualising surface water–groundwater exchange in braided river systems, *Hydrol. Earth Syst. Sci.*, 28, 2721–2743, <https://doi.org/10.5194/hess-28-2721-2024>, 2024.
- 835 Zhiteneva, V., Brune, J., Mischo, H., Weyer, J., Simon, A., and Lipson, D.: *Reiche Zeche Mine Water Geochemistry*, 2016.
- Zuecco, G., Penna, D., Borga, M., and Meerveld, H. J. van: A versatile index to characterize hysteresis between hydrological variables at the runoff event timescale, *Hydrol. Process.*, 30, 1449–1466, <https://doi.org/10.1002/hyp.10681>, 2016.